

# Quarkonia correlators and spectral functions from lattice QCD.

**Péter Petreczky**

Department of Physics and RIKEN-BNL Research Center, Brookhaven National Laboratory, Upton, New York, 11973

**Abstract.** I discuss recent progress in calculating quarkonia correlators and spectral functions on the lattice in relation with the problem of quarkonia dissolution at high temperatures and heavy quark transport in Quark Gluon Plasma.

PACS numbers: 11.15.Ha, 11.10.Wx, 12.38.Mh, 25.75.Nq

## 1. Introduction

Heavy quarkonia play an important role in studying hot and dense strongly interacting matter. Because of the heavy quark mass quarkonia binding can be understood in terms of the static potential. General considerations suggest that quarkonia could melt at temperatures above the deconfinement temperature as a result of modification of inter-quark forces (color screening). It has been conjectured by that melting of different quarkonia states due to color screening can signal Quark Gluon Plasma formation in heavy ion collisions [1]. Many studies of quarkonia dissolution rely heavily on potential models [2, 3, 4, 5, 6, 7]. However it is very unclear if such models are valid at finite temperature [8].

The problem of quarkonium dissolution can be studied more rigorously in terms of meson (quarkonium) spectral functions. Lattice calculation of charmonium spectral functions appeared recently and suggested, contrary to potential models, that  $J/\psi$  and  $\eta_c$  survive at temperatures as high as  $1.6T_c$  [9, 10, 11, 12]. It has been also found that  $\chi_c$  melts at temperature of about  $1.1T_c$  [11, 12, 13]. There are also preliminary calculations of the bottomonium spectral functions [14, 15].

## 2. Meson correlators and spectral functions

In lattice QCD we calculate correlators of point meson operators of the form

$$J_H(t, x) = \bar{q}(t, x)\Gamma_H q(t, x), \quad (1)$$

where  $\Gamma_H = 1, \gamma_5, \gamma_\mu, \gamma_5\gamma_\mu, \gamma_\mu\gamma_\nu$  and fixes the quantum number of the channel to scalar, pseudo-scalar, vector, axial-vector and tensor channels correspondingly. The relation of these quantum number channels to different meson states is given in Tab. 1.

| $\Gamma$              | $^{2S+1}L_J$ | $J^{PC}$ | $u\bar{u}$ | $c\bar{c}(n=1)$ | $c\bar{c}(n=2)$ | $b\bar{b}(n=1)$ | $b\bar{b}(n=2)$ |
|-----------------------|--------------|----------|------------|-----------------|-----------------|-----------------|-----------------|
| $\gamma_5$            | $^1S_0$      | $0^{-+}$ | $\pi$      | $\eta_c$        | $\eta'_c$       | $\eta_b$        | $\eta'_b$       |
| $\gamma_s$            | $^3S_1$      | $1^{--}$ | $\rho$     | $J/\psi$        | $\psi'$         | $\Upsilon(1S)$  | $\Upsilon(2S)$  |
| $\gamma_s\gamma_{s'}$ | $^1P_1$      | $1^{+-}$ | $b_1$      | $h_c$           |                 | $h_b$           |                 |
| 1                     | $^3P_0$      | $0^{++}$ | $a_0$      | $\chi_{c0}$     |                 | $\chi_{b0}(1P)$ | $\chi_{b0}(2P)$ |
| $\gamma_5\gamma_s$    | $^3P_1$      | $1^{++}$ | $a_1$      | $\chi_{c1}$     |                 | $\chi_{b1}(1P)$ | $\chi_{b1}(2P)$ |

**Table 1.** Meson states in different channels

Most dynamic properties of a finite temperature system are incorporated in the spectral function. The spectral function  $\sigma_H(p_0, \vec{p})$  for a given mesonic channel  $H$  in a system at temperature  $T$  can be defined through the Fourier transform of the real time two-point functions  $D^>$  and  $D^<$  or, equivalently, as the imaginary part of the Fourier transformed retarded correlation function [16],

$$\sigma_H(p_0, \vec{p}) = \frac{1}{2\pi}(D_H^>(p_0, \vec{p}) - D_H^<(p_0, \vec{p})) = \frac{1}{\pi} \text{Im} D_H^R(p_0, \vec{p}) \quad (2)$$

$$D_H^{>(<)}(p_0, \vec{p}) = \int \frac{d^4p}{(2\pi)^4} e^{ip \cdot x} D_H^{>(<)}(x_0, \vec{x}) \quad (3)$$

$$\begin{aligned} D_H^>(x_0, \vec{x}) &= \langle J_H(x_0, \vec{x}) J_H(0, \vec{0}) \rangle \\ D_H^<(x_0, \vec{x}) &= \langle J_H(0, \vec{0}) J_H(x_0, \vec{x}) \rangle, \quad x_0 > 0 \end{aligned} \quad (4)$$

The Euclidean time correlator calculated on the lattice

$$G_H(\tau, \vec{p}) = \int d^3x e^{i\vec{p} \cdot \vec{x}} \langle T_\tau J_H(\tau, \vec{x}) J_H(0, \vec{0}) \rangle \quad (5)$$

is an analytic continuation of the real time correlator  $G_H(\tau, \vec{p}) = D^>(-i\tau, \vec{p})$ .

Using this equation and the Kubo-Martin-Schwinger (KMS) condition [16] for the correlators

$$D_H^>(x_0, \vec{x}) = D^<(x_0 + i/T, \vec{x}), \quad (6)$$

one can relate the Euclidean propagator  $G_H(\tau, \vec{p})$  to the spectral function in Eq. (2), through the integral representation

$$\begin{aligned} G(\tau, \vec{p}) &= \int_0^\infty d\omega \sigma(\omega, \vec{p}) K(\omega, \tau) \\ K(\omega, \tau) &= \frac{\cosh(\omega(\tau - 1/2T))}{\sinh(\omega/2T)}. \end{aligned} \quad (7)$$

To reconstruct the spectral function from the lattice correlator  $G(\tau, T)$  this integral representation should be inverted. Since the number of data points is less than the number of degrees of freedom (which is  $\mathcal{O}(100)$  for reasonable discretization of the integral) spectral functions can be reconstructed only using the Maximum Entropy Method (MEM) [17]. In this method one looks for a spectral function which maximizes the conditional probability  $P[\sigma|DH]$  of having the spectral function  $\sigma$  given the data  $D$

and some prior knowledge  $H$  which for positive definite spectral function can be written as

$$P[\sigma|DH] = \exp(-\frac{1}{2}\chi^2 + \alpha S), \quad (8)$$

where

$$S = \int d\omega \left[ \sigma(\omega) - m(\omega) - \sigma(\omega) \ln\left(\frac{\sigma(\omega)}{m(\omega)}\right) \right] \quad (9)$$

is the Shannon - Janes entropy. The real function  $m(\omega)$  is called the default model and parametrizes all additional prior knowledge about the spectral functions, such as the asymptotic behavior at high energy [17]. In order to have sufficient number of data points either very fine isotropic lattices [11, 12, 15] or anisotropic lattices [9, 10, 13, 14] have been used.

### 3. Charmonia correlators and spectral functions

The spectral function for pseudo-scalar charmonium spectral functions calculated on anisotropic lattice [13] is shown in Fig. 1. The first peak in the spectral function corresponds to  $\eta_c(1S)$  state. The position of the peak and the corresponding amplitude (i.e. the area under the peak) are in good agreement with the results of simple exponential fit. The second peak in the spectral function is most likely the combination of several excited states as its position and amplitude is higher than what one would expect for pure 2S state. The spectral function becomes sensitive to the effects of the finite lattice spacings for  $\omega > 5\text{GeV}$ . In this  $\omega$  region the spectral functions becomes also sensitive to the choice of the default model. This is because only a very few data points in the correlator carry information about the spectral function in the region  $\omega > 5\text{GeV}$ .

Also shown in Fig.1 is the spectral function in the scalar channel from Ref. [13]. The 1st peak corresponds to  $\chi_{c0}(1P)$  state. The correlator is more noisy in the scalar channel than in the pseudo-scalar one. As the results the  $\chi_{c0}(1P)$  peak is less pronounced and has larger statistical errors. The peak position and the area under the peak is consistent with the simple exponential fit. As in the pseudo-scalar case individual excited states are not resolved and the spectral function depends on the lattice spacing and default model for  $\omega > 5\text{GeV}$ . Similar results have been found for the vector and axial-vector channels which correspond to  $J/\psi$  and  $\chi_{c1}$  states respectively.

We would like to know what happens to different charmonia states at temperatures above the deconfinement temperature  $T_c$ . With increasing temperature it becomes more and more difficult to reconstruct the spectral functions as both the number of available data points as well as the physical extent of the time direction (which is  $1/T$ ) decreases. Therefore it is useful to study the temperature dependence of charmonia correlators first. From Eq. (7) it is clear that the temperature dependence of charmonia correlators come from two sources: the temperature dependence of the spectral function and the temperature dependence of the integration kernel  $K(\tau, \omega, T)$ . To separate out the trivial

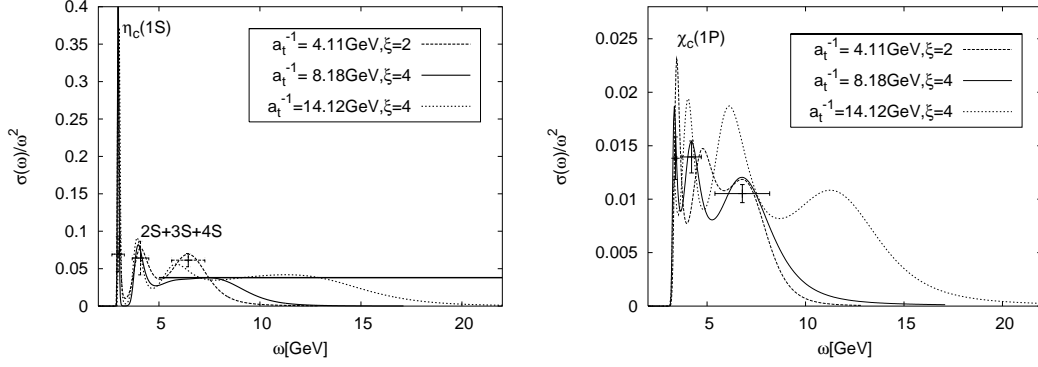


**Figure 1.** Charmonium spectral function in the pseudo-scalar channel (left) and the scalar channel (right) at different lattice spacings and zero temperature from Ref. [13].  $m(\omega) = 1$  was used as the default model.

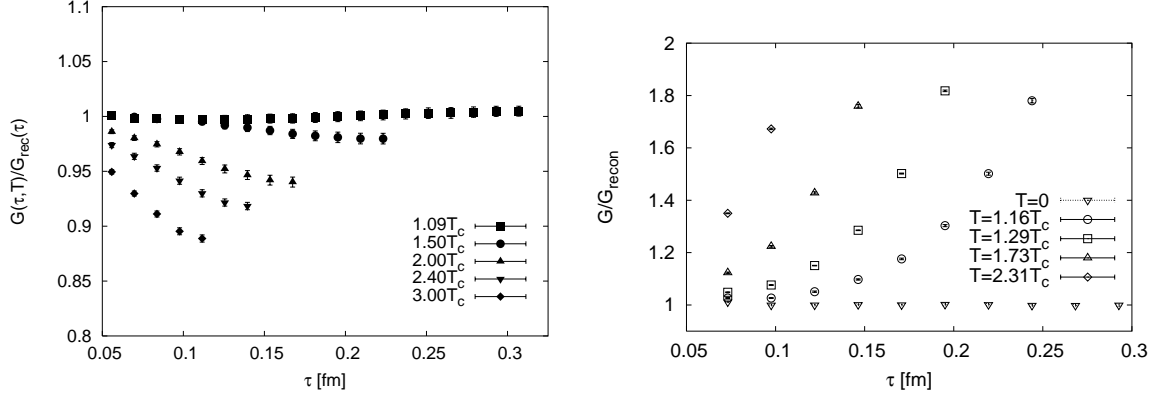


**Figure 2.** The ratio  $G(\tau, T)/G_{recon}(\tau, T)$  of charmonium for pseudoscalar channel at at  $a_t^{-2} = 14.11\text{GeV}$  (left) and scalar channel at at  $a_t^{-2} = 8.18\text{GeV}$  (right) at different temperatures [13].

temperature dependence due to the integration kernel, following Ref. [12] for each temperature we calculate the so-called reconstructed correlator

$$G_{recon}(\tau, T) = \int_0^\infty d\omega \sigma(\omega, T=0) K(\tau, \omega, T). \quad (10)$$

Now if we assume that there is no temperature dependence in the spectral function, then the ratio of the original and the reconstructed correlator should be close to one,  $G(\tau, T)/G_{recon}(\tau, T) \sim 1$ . This way we can identify the cases when spectral function itself changes dramatically with temperature. This gives reliable information about the fate of charmonia states above deconfinement. In Fig. 2 we show this ratio for pseudo-scalar and scalar channels correspondingly calculated on anisotropic lattice [13]. From the figures one can see that the pseudo-scalar correlators shows only very small changes till  $1.5T_c$  indicating that the  $\eta_c$  state survives till this temperature with little modification of its properties. On the other hand the scalar correlator shows large changes already at  $1.16T_c$  suggesting strong modification or dissolution of the  $\chi_{c0}$  state at this temperature.

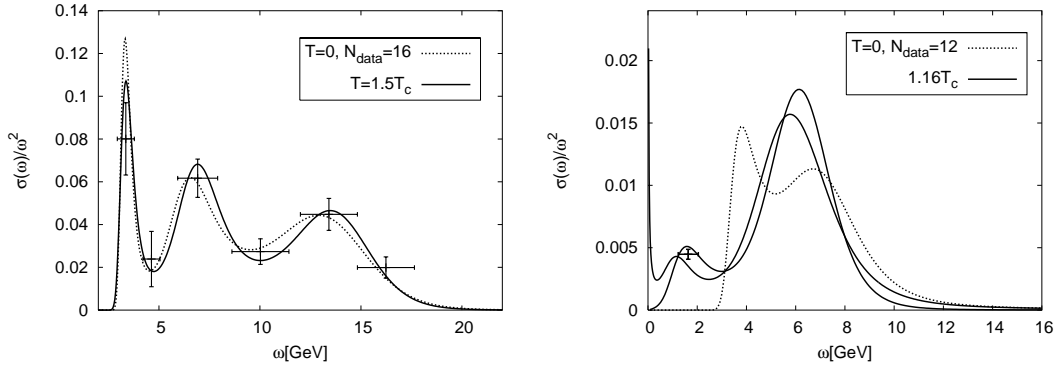


**Figure 3.** Charmonia spectral function in the pseudoscalar channel at  $a_t^{-2} = 14.11\text{GeV}$  (left) and the scalar channel (right) at  $a_t^{-2} = 8.18\text{GeV}$  for zero and finite temperature [13]. In the pseudo-scalar channel  $m(\omega) = 0.1$  has been used as the default model. In the scalar channel we have used  $m(\omega) = 0.038\omega^2$  as the default model as well as  $m(\omega) = 1$  for  $T = 1.16T_c$ .

More detailed information on different charmonia states at finite temperature can be obtained by calculating spectral functions using MEM. The results of these calculations are shown in Figs. 3. Because at high temperature the temporal extent and the number of data points where the correlators are calculated become smaller the spectral functions reconstructed using MEM are less reliable. To take into account possible systematic effects when studying the temperature modifications of the spectral functions we compare the finite temperature spectral functions against the zero temperature spectral functions obtained from the correlator using the same time interval and number of data points as available at finite temperature. We see that spectral functions in the pseudo-scalar channel show no temperature dependence within the statistical errors. This is in accord with the analysis of the correlation functions. Also the spectral functions show very little dependence on the default model. Similar conclusion has been made in Ref. [11, 12] where correlators and spectral functions have been calculated on very fine isotropic lattices as well as in Ref. [10] where anisotropic lattices have been used. The pseudo-scalar spectral function was found to be temperature independent also in Ref. [9] where correlators of extended meson operators have been studied on anisotropic lattices. The study of the charmonium correlators with different spatial boundary conditions provides further evidence for survival of the  $1S$  charmonia states well above the deconfinement transition temperature [18].

The scalar spectral function shows large changes at  $1.16T_c$  which is consistent with correlator-based analysis. Also default model dependence of the scalar correlator is large above the deconfinement transition (c.f. Fig. 3, right). This means that the  $\chi_{c0}$  ( $^3P_0$ ) dissolves at this temperature. Similar results for the scalar spectral function have been reported in [11, 12]. The results for the axial correlators and spectral functions are similar to scalar ones [12] as expected.

The vector correlator, however, has temperature dependence different from that of the pseudo-scalar channel [19]. This is due to the fact that the vector current is

conserved and there is a contribution to spectral functions at very small energy  $\omega \simeq 0$  corresponding to heavy quark transport [20, 21]. The transport peak in the spectral functions can be written as [20]

$$\sigma_{low}(\omega) = \chi_s(T) \frac{T}{M} \frac{1}{\pi} \frac{\omega\eta}{\omega^2 + \eta^2}, \quad (11)$$

where  $\eta = T/(MD)$  with  $D$  being the heavy quark diffusion constant. Furthermore  $\chi_s(T)$  is the charm or beauty susceptibility and  $M$  is the heavy quark mass. To the first approximation the transport contribution to the spectral function gives rise to a positive constant contribution to the correlator  $G_{low}(\tau) \simeq \chi_s(T)T^2/M$  [20] resulting in an enhancement of the finite temperature correlators relative to the zero temperature ones, in agreement with the lattice data presented in [19, 22]. Finite value of the diffusion constant  $D$  will give rise to some curvature in  $G_{low}(\tau)$ . The smaller the value of  $D$  is, the larger is the curvature in  $G_{low}(\tau)$ . Thus extracting  $G_{low}(\tau)$  from lattice data and estimating its curvature can give an estimate for  $D$ . This, however, requires very precise lattice data which are not yet available [20].

#### 4. Bottomonium correlators and spectral functions

Bottomonium correlators and spectral functions have also been studied using anisotropic [14] as well as very fine isotropic lattice with lattice spacing  $a^{-1} = 9.72\text{GeV}$  [15]. These studies, however, are far less detailed than the charmonium studies presented above and are still preliminary. In Fig. 4 the temperature dependence of the ratio  $G/G_{recon}$  is shown for pseudo-scalar channel at different temperatures calculated using anisotropic lattices. This ratio shows almost no temperature dependence till  $2.3T_c$ . This is expected as the pseudo-scalar  $1S$  bottomonium state, the  $\eta_b$ , is much smaller than the corresponding charmonium state, thus survives till much higher temperatures. Also shown in Fig. 4 is the pseudo-scalar function at different temperatures. The first peak corresponds to the  $\eta_b$  state and survives above the deconfinement temperature in agreement with the analysis of the correlation functions. Other peaks are artifacts of the finite lattice spacing and MEM analysis.

An interesting question is what happens to  $1P$  bottomonia states. They have sizes similar to the  $1S$  charmonia states and thus are expected to survive in the deconfined phase till temperatures of about  $1.5T_c$ . In Fig. 5 I show the temperature dependence of  $G/G_{recon}$  in the scalar channel corresponding to  $\chi_{b0}$ . As one can see from the figure the scalar correlator shows dramatic change across the deconfinement temperature and its behavior is similar to the behavior of the scalar correlator in the charmonium case. Also shown in Fig. 5 is the bottomonium spectral functions in the scalar channel. Contrary to the pseudo-scalar channel the scalar spectral function shows significant changes above the deconfinement temperature and therefore it seems that the  $\chi_b$  state is strongly modified or even dissolved at  $1.15T_c < T < 1.5T_c$ . Lattice calculations presented in Ref. [15] show similar results. In particular, they also show large increase of the scalar

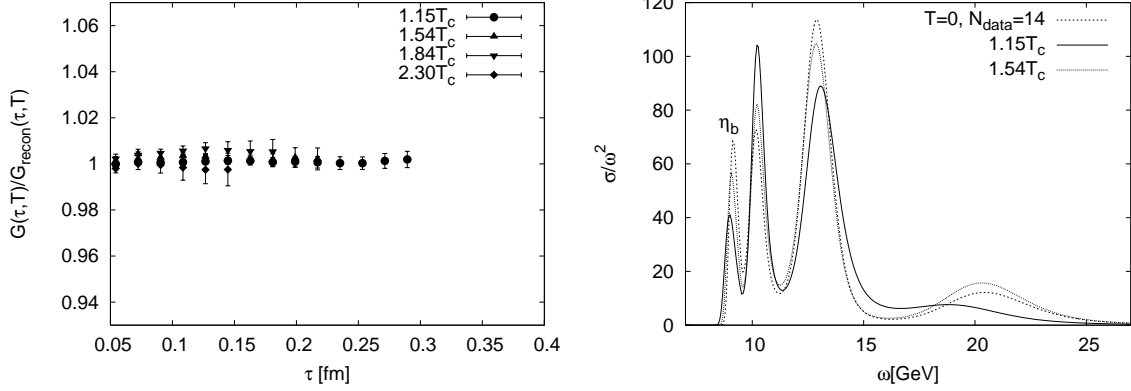


**Figure 4.** Bottomonia correlators (left) spectral functions (right) in pseudo-scalar channel for different temperatures from Ref. [14].

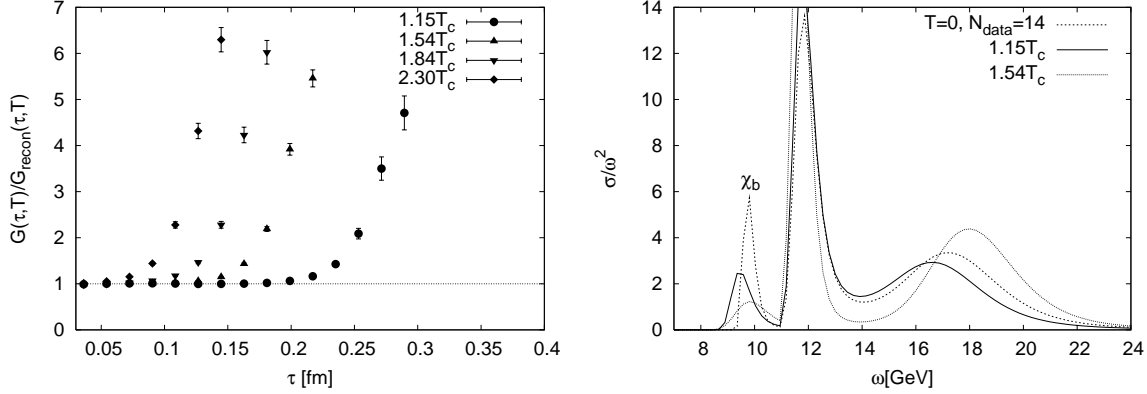


**Figure 5.** Bottomonia correlators (left) spectral functions (right) in scalar channel for different temperatures from Ref. [14].

bottomonium correlator and strong modification of the corresponding spectral function.

## 5. Conclusions

In this contribution it has been shown how lattice calculation can provide information on quarkonia properties at finite temperature. The temperature dependence of the pseudo-scalar correlators as well as the spectral functions extracted using MEM shows that the  $1S$  charmonia states exist as a resonance in the deconfined phase till temperatures as high as  $1.5T_c$ . On the other hand lattice calculation show that the  $1P$  charmonia states dissolve at  $T \sim 1.1T_c$ . Study of the bottomonia at finite temperature is also in progress [14, 15]. It should be stressed that all lattice calculation discussed so far have been done in quenched approximation, i.e. neglecting the effect of sea quarks. To make contact with heavy ion experiments certainly the effect of the sea quarks has to be included, but computationally this is very expensive. Recent attempts to study charmonia properties at finite temperature in full QCD (i.e. with sea quarks) are reported in Ref. [23]. The

findings of Ref. [23] are consistent with the quenched results.

Recent studies of quarkonium properties at finite temperature using potential model claim agreement with the lattice data [5, 6, 7]. The dissociation temperature of different quarkonia states quoted in these studies and defined as temperature where binding energy becomes zero is indeed significantly higher than before. However, potential models with screened potential also predict modification of quarkonia properties, which in turn lead to changes in the spectral function and correlators. Such changes are not observed in the lattice correlator [21, 24]. Thus it is not clear at the moment whether modification of quarkonia properties at finite temperature can be understood in terms of a screened temperature dependent heavy quark potential.

## 6. Acknowledgments

This work was supported by U.S. Department of Energy under Contract No. DE-AC02-98CH10886 as well as by LDRD funds.

- [1] T. Matsui and H. Satz, Phys. Lett. B **178**, 416 (1986)
- [2] F. Karsch, M. T. Mehr and H. Satz, Z. Phys. C **37**, 617 (1988)
- [3] S. Digal, P. Petreczky and H. Satz, Phys. Lett. B **514**, 57 (2001)
- [4] S. Digal, P. Petreczky and H. Satz, Phys. Rev. D **64**, 094015 (2001)
- [5] E. V. Shuryak and I. Zahed, Phys. Rev. D **70**, 054507 (2004)
- [6] C. Y. L. Wong, Phys. Rev. C **72**, 034906 (2005)
- [7] W. M. Alberico, A. Beraudo, A. De Pace and A. Molinari, Phys. Rev. D **72**, 114011 (2005)
- [8] P. Petreczky, Eur. Phys. J. C **43**, 51 (2005)
- [9] T. Umeda, K. Nomura and H. Matsufuru, hep-lat/0211003
- [10] M. Asakawa and T. Hatsuda, Phys. Rev. Lett. **92**, 012001 (2004)
- [11] S. Datta, F. Karsch, P. Petreczky and I. Wetzorke, hep-lat/0208012
- [12] S. Datta, F. Karsch, P. Petreczky and I. Wetzorke, Phys. Rev. D **69**, 094507 (2004)
- [13] A. Jakovác, P. Petreczky, K. Petrov and A. Velytsky, hep-lat/0603005; work in progress
- [14] K. Petrov, A. Jakovác, P. Petreczky, A. Velytsky, PoS (LAT2005), 153 (2005)
- [15] S. Datta, A. Jakovác, F. Karsch and P. Petreczky, hep-lat/0603002
- [16] M. Le Bellac, *Thermal Field Theory*, Cambridge University Press, 1996
- [17] M. Asakawa, T. Hatsuda and Y. Nakahara, Prog. Part. Nucl. Phys. **46**, 459 (2001)
- [18] H. Iida, T. Doi, N. Ishii, H. Suganuma and K. Tsumura, hep-lat/0602008
- [19] P. Petreczky, K. Petrov, D. Teaney, A. Velytsky, hep-lat/0510021
- [20] P. Petreczky, D. Teaney, Phys. Rev. D **73**, 014508 (2006)
- [21] Á. Mócsy, P. Petreczky, Eur. Phys. J. C **43**, 77 (2005), Phys. Rev. D **73**, 074007 (2006)
- [22] S. Datta, F. Karsch, S. Wissel, P. Petreczky and I. Wetzorke, hep-lat/0409147
- [23] R. Morrin, A. P. O Cais, M. B. Oktay, M. J. Peardon, J. I. Skullerud, G. Aarts and C. R. Allton, hep-lat/0509115
- [24] Á. Mócsy, contribution to this proceeding